Vibrational lifetimes and vibrational line positions in polyatomic supercritical fluids near the critical point

R. S. Urdahl, D. J. Myers, K. D. Rector, P. H. Davis, B. J. Cherayil,[a] and M. D. Fayer
Department of Chemistry, Stanford University, Stanford, California 94305

(Received 10 April 1997; accepted 4 June 1997)

Picosecond infrared pump–probe experiments are used to measure the vibrational lifetime of the asymmetric (T_{1u}) CO stretching mode of $W(CO)_6$ in supercritical CO_2, C_2H_6, and CHF_3 as a function of solvent density and temperature. As the density is increased at constant temperature from low, gaslike densities, the lifetimes become shorter. However, in all three solvents, it is found that within a few degrees of the critical temperature ($T_r \equiv T/T_c \approx 1.01$), the lifetimes are essentially constant over a wide range of densities around the critical value (ρ_c). When the density is increased well past ρ_c, the lifetimes shorten further. At higher temperature ($T_r = 1.06$) this region of constant vibrational lifetime is absent. Infrared absorption spectra of $W(CO)_6$ and $Rh(CO)_2$acac in supercritical CO_2, C_2H_6, and CHF_3 acquired for the same isotherms show that the vibrational spectral peak shifts follow similar trends with density. The peak positions shift to lower energy as the density is increased. Near the critical point, the peak positions are density independent, and then redshift further at densities well above ρ_c. It is shown that critical fluctuations play a dominant role in the observed effects. Theoretical calculations ascribe the density independence of the observables to the cancellation of various rapidly changing quantities near the critical point. The theory's calculation of density independence implicitly involves averages over all local densities and does not involve any form of solute–solvent clustering. © *1997 American Institute of Physics.* [S0021-9606(97)50834-8]

I. INTRODUCTION

Supercritical fluids are a useful medium for the study of chemical dynamics because the density can be continuously varied from values characteristic of a gas to those characteristic of a liquid. For temperatures at or above the critical temperature, T_c, this large range of densities is accessible without the occurrence of discontinuities in physical properties associated with the first-order phase changes such as vaporization or condensation. Although the bulk properties of coexisting phases merge at the critical point, long correlation length density variations around the critical pressure (P_c) and at or slightly above the critical temperature (T_c) cause singularities in many thermodynamic functions. One notable consequence of the long correlation length is the phenomenon of critical opalescence, where variations in the refractive index result in the anomalous scattering of light.

The transition from a dilute gas to a compressed liquid is accomplished by distinct changes in the nature of the molecular interactions. For a molecule in a low-density gas, the surrounding molecules behave as a set of random scatterers, and the dynamics are determined by a series of uncorrelated binary collisions. At high densities, the molecule interacts continuously with a large number of nearest neighbors, and collisions are no longer uncorrelated. A detailed microscopic picture of the dynamics spanning the range of densities *intermediate* to these limits is an important goal in the study of relaxation phenomena in supercritical fluids.

In this paper, we report measurements of the vibrational lifetimes and vibrational spectral peak positions of polyatomic solutes in several polyatomic supercritical fluids over a wide range of densities, including the critical density ρ_c, at temperatures very close to T_c.[1] The vibrational lifetimes of the T_{1u} asymmetric CO stretching mode of tungsten hexacarbonyl ($W(CO)_6$) in three supercritical fluids (SCFs), carbon dioxide, ethane, and fluoroform, were measured as a function of density along isotherms from 2 deg above T_c up to 20 deg above T_c. In addition, the spectral peak positions of both $W(CO)_6$ and rhodium dicarbonylacetylacetonate ($Rh(CO)_2$acac) were measured in the same SCFs as a function of density at the same temperatures. Near T_c, for a wide range of densities about ρ_c, the lifetime data display a striking dependence on density. As the density is increased from about 1 mol/L, the lifetime decreases. However, as ρ_c is approached, the lifetime becomes density independent. The density independent region spans approximately a factor of two change in density. At sufficiently high density, the lifetime again decreases with increasing density. The spectral peak positions display a similar density dependence. As the density is increased from low density, the peak positions of both $W(CO)_6$ and $Rh(CO)_2$acac shift to lower energy (redshift). In the region around ρ_c, the peak positions become density independent. As the density is increased well beyond ρ_c, the peak positions redshift further. This very pronounced plateau in the redshift is absent once the temperature is raised about 20 deg above T_c.

A theory of the temperature and density dependence of vibrational lifetimes and peak positions has recently been developed using density functional methods.[2] As discussed below, the theory allows vibrational observables to be ex-

[a]On leave from the Department of Inorganic and Physical Chemistry, Indian Institute of Science, Bangalore-560012, India.

pressed in terms of thermodynamic functions and can be used in both the critical and noncritical limits. It also provides a framework for identifying the physical phenomena that are responsible for anomalous behavior. The results are rather surprising. Near the critical point, as a result of the divergence of the correlation length of the density fluctuations, factors that could potentially lead to density dependent frequencies and lifetimes scale out of the problem. The calculations implicitly involve averages over all local densities. The density independence of the observables arising from the theoretical calculations does not depend on any form of solute–solvent clustering.

Early thermodynamic measurements in SCFs suggested that the local solvent density about a solute at infinite dilution is a sensitive function of temperature and pressure near the critical point.[3,4] Several molecular-level experimental studies[5–7] of solute-solvent interactions in infinitely dilute SCFs have identified three distinct density regimes for solvation, which are most pronounced along isotherms slightly above T_c; they are somewhat loosely defined as the low-density, gaslike region ($\rho_r<0.5$), the near-critical region ($0.5<\rho_r<1.5$), and the high-density, liquidlike region ($\rho_r>1.5$). Further discussion of these experiments is given in Sec. VI.

The utility of ultrafast time-resolved spectroscopies in studying microscopic molecular dynamics in supercritical fluids was demonstrated by work from Hochstrasser's laboratory[8] on the isomerization of *trans*-stilbene in supercritical ethane. Near $P_r \equiv P/P_c = 1$, $T_r = 1.15$, the electronic excited-state lifetime of *trans*-stilbene is essentially constant over roughly a factor of 2 change in the pressure. This result was interpreted as suggesting the formation of clusters sufficiently large that their local properties were independent of the bulk density.

Harris and co-workers studied the electronic excitation, dissociation, and recombination of I_2 in supercritical rare gas solvents, and examined the process of vibrational cooling on the ground state potential surface as a function of density and temperature far from the critical point.[9–12] Zewail and co-workers measured coherent vibrational wave packet dynamics in the excited state of I_2 in rare gas SCFs as a function of density at room temperature.[13–15] Troe and co-workers[16] have studied the rate constants for vibrational deactivation of electronically excited azulene in supercritical helium, xenon, nitrogen, ethane, and carbon dioxide over a wide range of densities at temperatures well above the critical isotherms.

The present experiments investigate vibrational dynamics and solute–solvent interactions in supercritical fluids, and explicitly consider the role of the length scale of density fluctuations on vibrational observables near the critical point. In contrast to previous vibrational experiments, ps ir pulses are used to excite vibrations and directly probe vibrational dynamics on the ground state potential surface. By exciting and probing the $v=0-1$ transition, the influences of density and temperature on the vibrational lifetime are investigated near the critical point.

II. EXPERIMENTAL PROCEDURES

The apparatus used to perform vibrational relaxation experiments in supercritical fluids consists of a picosecond midinfrared laser system and a variable-temperature, high-pressure optical cell. The laser system is a slightly modified version of a design previously described in detail[17] and will only be briefly discussed here. An output-coupled, acousto-optically Q-switched and mode-locked Nd:YAG laser is used to synchronously pump a Rh610 dye laser. A cavity-dumped 1.06 μm pulse is doubled to give $\sim$600 μJ of light at 532 nm with a pulse width of $\sim$70 ps. The output pulse from the amplified dye laser ($\sim$30–40 μJ@595 nm, 40 ps) and the cavity-dumped, frequency-doubled pulse at 532 nm serve as the signal and pump inputs, respectively, in a $LiIO_3$ optical parametric amplifier (OPA) used to generate the idler output near 5 μm. The ir wavelength is determined to within ± 0.25 cm^{-1} using a FTIR spectrometer.

The ir pulse ($\sim$2 μJ) is split into a weak probe beam, which passes down a computer controlled variable delay line with up to 5 ns of delay, and a strong pump beam. The pump and probe pulses are counter propagating and focused into the center of the SCF cell. Typical spot sizes (1/*e* radius of **E** field) were $\omega_0 \sim 140$ μm for the pump beam and $\omega_0 \sim 60$ μm for probe beam. A few percent of the transmitted probe beam is split off and directed onto an InSb detector (Electro-Optical Systems). The signal from the pump–probe experiment is measured with a set of electronics that does shot-to-shot normalization and lock-in detection at the experimental repetition rate of 900 Hz, and is recorded by computer.

The high-pressure optical cell is comprised of a Monel 400 body, gold or Teflon O-rings, and CaF_2 or sapphire windows. The two windows are secured using an opposed force type seal incorporating Belleville spring washers. Stable temperatures are produced using coaxial heating cable (Philips Thermocoax) together with a fuzzy-logic controller/power supply (Solitech). Two 100 Ω platinum resistance temperature detectors (RTD's) are inserted in the body of the cell to permit careful measurement and control of the temperature to within ± 0.2 °C. A syringe pump (Isco 100-DX) was used to generate the variable pressures required to compress the fluid to the desire density. The pressure was accurately monitored to less than ± 1 psia with a precision strain-gauge transducer (Sensotech).

The experiments were conducted on the asymmetric CO stretching mode of $W(CO)_6$ near 1990 cm^{-1} (5.03 μm) and the symmetric CO stretch of $Rh(CO)_2acac$ around 2090 cm^{-1} (4.78 μm). The concentrations were $\sim 10^{-5}$ mol/L. The laser frequency was tuned to the absorption peak at each density. A typical sample was prepared by placing a few micrograms of solid $W(CO)_6$ (Aldrich, 99%) or $Rh(CO)_2acac$ (Aldrich, 99%) on the tip of a syringe needle, inserting the powder into the center of the SCF cell through a sideport, and then compressing the system to the final operating pressure with high-purity CO_2 (Middleton Bay Airgas, 99.9995%; $T_c = 304.1$ K, $P_c = 1070$ psia, $\rho_c = 10.63$ mol/L), ethane (Byrne Specialty Gases, 99.99%; $T_c = 305.4$ K, $P_c = 706$ psia, $\rho_c = 6.87$ mol/L) or fluoroform (Scott Spe-

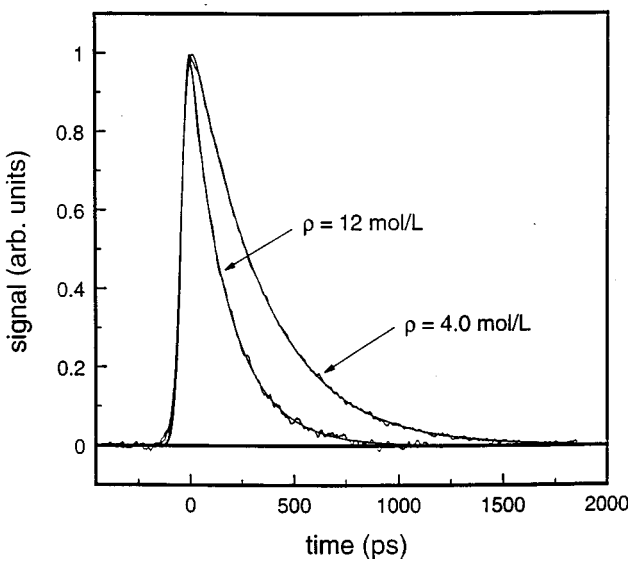

FIG. 1. Typical infrared pump–probe decay for the T_{1u} asymmetric CO stretch of $W(CO)_6$ in supercritical ethane at 34 °C. The lines through the data represent fits obtained by convolving the instrument response with an exponential decay. The lifetime (T_1) of the data at 4.0 mol/L is 315 ps; the 12.0 mol/L data fits to a value of $T_1=185$ ps.

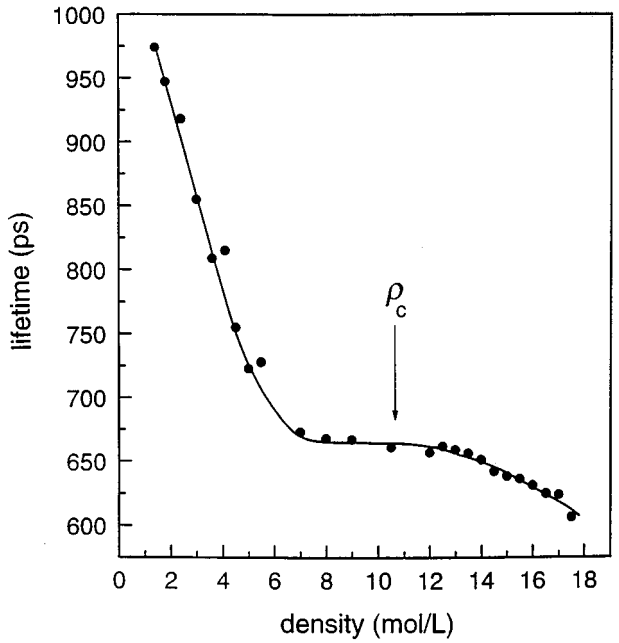

FIG. 2. Vibrational lifetime of the T_{1u} asymmetric CO stretching mode of $W(CO)_6$ versus density of CO_2 at 33 °C ($T_r\approx1.01$). The line through the data is a visual aid. For a range of densities roughly centered about ρ_c (marked with an arrow), the vibrational lifetime forms a density-independent plateau. The critical temperature is 31 °C and the critical density is 10.63 mol/L.

cialty Gases, 99.9%; $T_c=299.1$ K, $P_c=699$ psia, $\rho_c=7.56$ mol/L). The SCF cell was flushed repeatedly with gas before final pressurization to eliminate any air introduced into the system during insertion of the solid solute.

The optical density of the sample was varied by repeatedly diluting the mixture with fresh gas until a value of roughly 0.8–1.2 was obtained; in some cases, scans were acquired with OD's as low as ~0.1. Absorbance measurements were made directly in the cell using a Mattson Research Series FTIR spectrometer (0.25 cm^{-1} resolution) configured for external beam operation. The optical layout makes it possible to easily switch from making ps pump–probe measurements to recording an ir spectrum.

Vibrational lifetimes were obtained by fitting the data to a convolution of the instrument response and an exponential using a grid-search fit method. Vibrational peak positions were obtained by subtracting a background spectrum of the pure SCF, taken at the experimental pressure and temperature, from the solute-solvent sample spectrum. This technique removes small solvent peaks that can distort the spectrum.

III. RESULTS

A. Vibrational lifetimes

Figure 1 shows typical lifetime data taken for $W(CO)_6$ in ethane at densities of 4.0 and 12.0 mol/L along the 34 °C isotherm. The lines through the data are the fits to the convolution of the instrument response with exponentials. Data of this quality were taken on all samples. Very high quality data are necessary to make the types of observations discussed below.

Isothermal plots of the vibrational lifetime versus solvent density at different reduced temperatures are given in Figs. 2 and 3 for $W(CO)_6$ in supercritical carbon dioxide. Figure 2 shows the changes in the vibrational lifetime over a factor of ~17 in density at 33 °C, $T_r\approx1.01$. From 1 to ~7 mol/L, the lifetime decreases smoothly and nonlinearly with

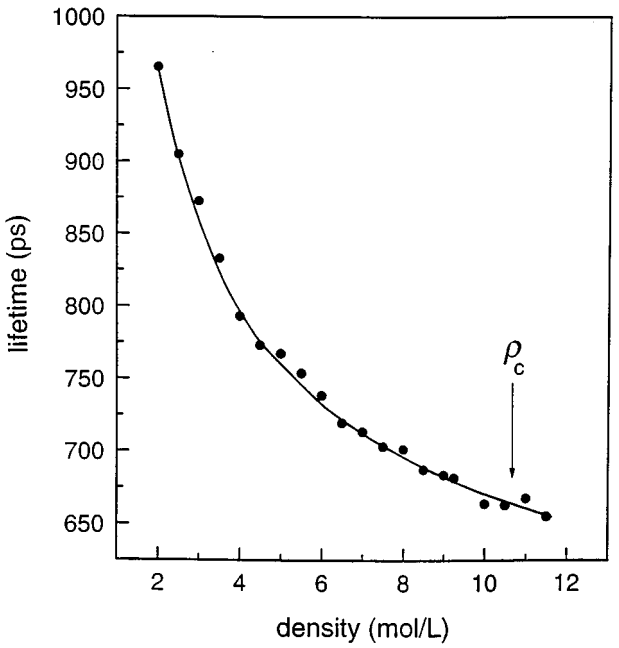

FIG. 3. Vibrational lifetime of the T_{1u} asymmetric CO stretching mode of $W(CO)_6$ versus density of CO_2 at 50 °C ($T_r=1.06$). The line through the data is a visual aid. Note that the lifetime now varies continuously with density. The critical density is marked with an arrow.

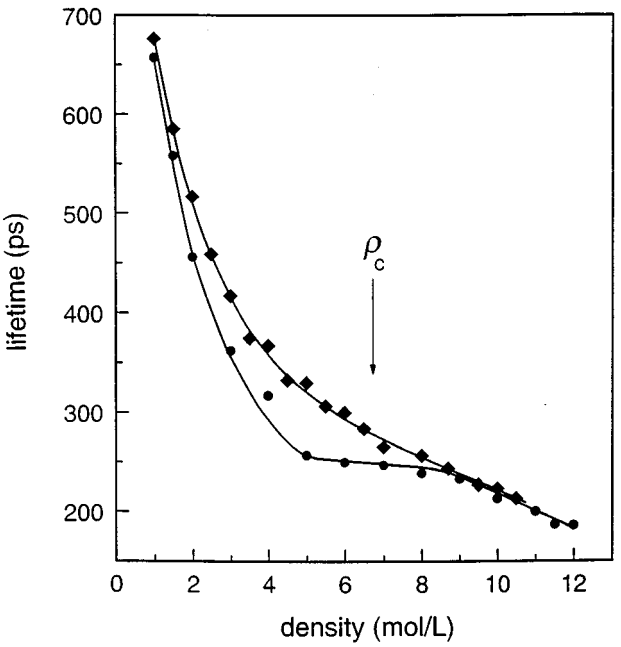

FIG. 4. Vibrational lifetime of the T_{1u} asymmetric CO stretching mode of $W(CO)_6$ versus density of C_2H_6 at 34 °C (circles; $T_r \approx 1.01$) and 50 °C (diamonds; $T_r = 1.06$). The lines through the data are intended to be a visual aid. A plateau region centered near ρ_c is the most prominent feature of the 34 °C data. In contrast, the vibrational lifetime changes smoothly with density along the 50 °C isotherm. These types of behavior are similar to that seen in Figs. 2 and 3 for CO_2. The critical temperature for ethane is 32.2 °C and the critical density (marked with an arrow) is 6.87 mol/L.

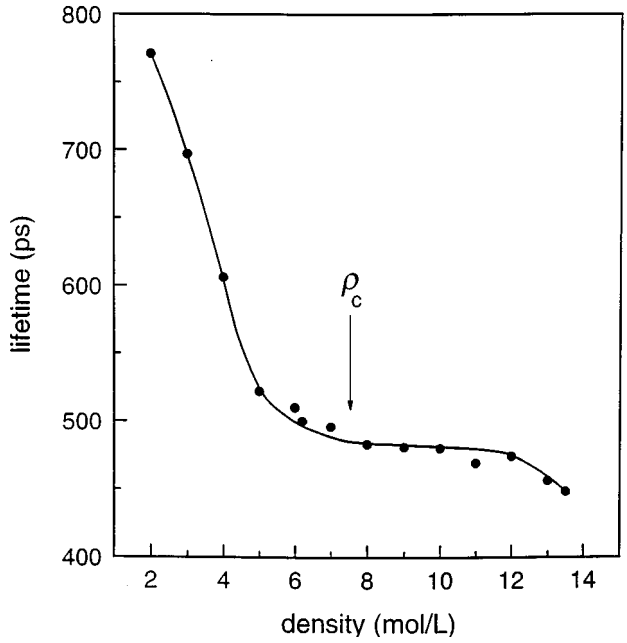

FIG. 5. Vibrational lifetime of the T_{1u} asymmetric CO stretching mode of $W(CO)_6$ versus density of CHF_3 at 28 °C ($T_r \approx 1.01$). The line through the data is a visual aid. The density-independent behavior of the lifetimes, seen earlier in Figs. 2 and 4 for CO_2 and C_2H_6, respectively, is visible here as well. Note that the plateau region is not symmetrical with respect to ρ_c. The critical temperature for fluoroform is 26.0 °C and the critical density (marked with an arrow) is 7.56 mol/L.

increasing density. In the intermediate range of densities from ~7–13 mol/L, the vibrational lifetime displays a plateau, i.e., it is independent of density. This plateau region ends around 13–14 mol/L. At higher densities, the lifetime gradually decreases. In the plateau, the lifetime remains constant although the density changes by nearly a factor of 2. A plot of CO vibrational lifetime vs density of CO_2 along the 50 °C isotherm ($T_r = 1.06$) is given in Fig. 3. The departure from the behavior observed at 33 °C is readily apparent; the lifetime varies smoothly across the range of densities studied, and there is no indication of a plateau region about the critical density. Comparison of Figs. 2 and 3 shows the dramatic effect that a change in temperature of 17 °C has on the nature of the density dependence of the vibrational lifetime.

Similar types of data sets have been acquired for $W(CO)_6$/ethane and $W(CO)_6/CHF_3$. Vibrational relaxation data for $W(CO)_6$ along the 34 °C ($T_r \approx 1.01$) and 50 °C ($T_r = 1.06$) isotherms of supercritical ethane are shown in Fig. 4. The lifetime vs density trends seen here correlate closely with those observed in the $W(CO)_6/CO_2$ system. Again, near the critical point, there is a plateau in the lifetime vs density plot. On the 50 °C isotherm, the plateau does not occur. Although the general shapes of the curves are similar in CO_2 and ethane, there are some important differences that should be noted. The lifetime is approximately a factor of 3 longer for $W(CO)_6/CO_2$ compared to $W(CO)_6$/ethane at all densities studied. The change in the vibrational lifetime with solvent confirms that the relaxation proceeds via intermolecular pathways that involve molecular vibrational modes of the SCF and/or collective solvent modes [instantaneous normal modes (INM) or phonons] of the fluid.[18–20]

The plateaus are approximately centered around 10 and 6.5 mol/L for CO_2 and ethane, respectively, which are approximately their critical densities. At a reduced temperature of ≈1.01, the region of constant vibrational lifetime in CO_2 (defined as that region of density over which τ changes by less than a few percent) is seen from Fig. 2 to extend from roughly 7.5–13 mol/L, i.e., $P_r = 0.70–1.2$. In supercritical ethane at 34 °C, Fig. 4 shows that the plateau region is again centered near ρ_c and extends over the range of ~5–8 mol/L, or $P_r = 0.75–1.2$. Thus the densities and widths of the plateau regions relative to ρ_c are very similar in the two systems.

The density dependence of the CO vibrational lifetime of $W(CO)_6$ in supercritical fluoroform is given in Fig. 5 at 28 °C, which corresponds to a reduced density of ≈1.01. The general shape of the curve is very similar to that seen for CO_2 and ethane, with a pronounced plateau region from ~7–12 mol/L. The magnitude of the lifetime in the plateau region (~480 ps) is intermediate between the plateau values in CO_2 (~660 ps) and ethane (~250) ps. The data in fluoroform shows the plateau occurs in a polar solvent as well as in nonpolar solvents. However, in fluoroform, the plateau does not appear to be symmetrical about ρ_c.

In Sec. IV, the vibrational lifetime data will be discussed in terms of the density functional calculations of the force correlation function. The importance of this approach is that

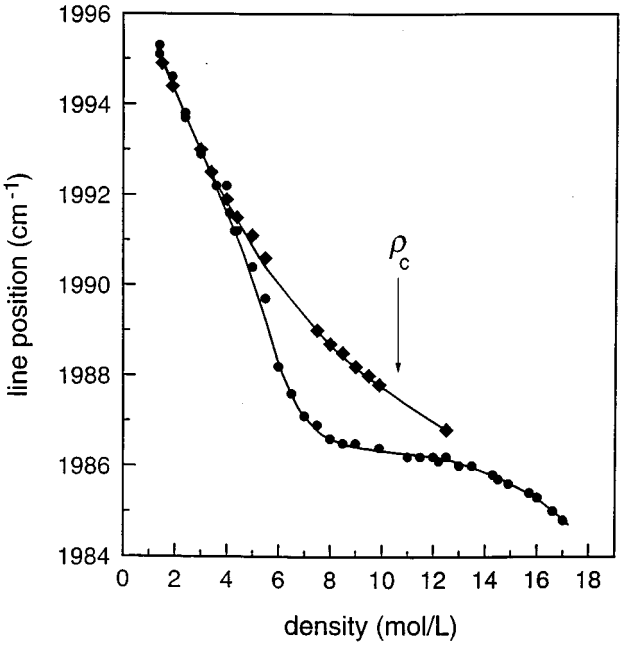

FIG. 6. Absorption line peak position of the T_{1u} asymmetric CO stretching mode of $W(CO)_6$ versus density of CO_2 at 33 °C (circles) and 50 °C (diamonds). The lines through the data are a visual aid, and the critical density is marked with an arrow. The vibrational line peak position data shown here display the same characteristic features apparent in all of the lifetime vs density plots, i.e., a plateau region in the observable occurring near the critical density along the $T_r \approx 1.01$ isotherm, and a continuous variation in this same parameter with density upon raising the temperature less than 20 °C.

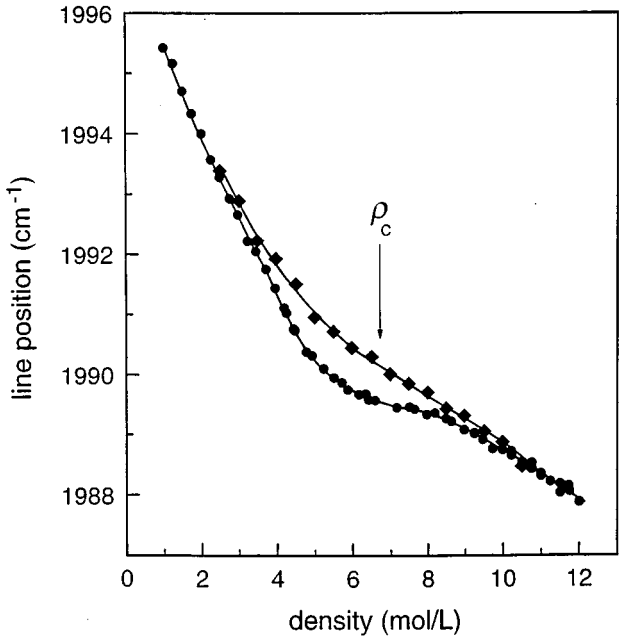

FIG. 7. Absorption line peak position of the T_{1u} asymmetric CO stretching mode of $W(CO)_6$ versus density of C_2H_6 at 34 °C (circles) and 50 °C (diamonds). The lines through the data are a visual aid. The critical density is marked by an arrow.

it is capable of describing vibrational relaxation both near and far from the critical point, where the key difference is the correlation length of the density fluctuations. These calculations will show that the existence of a plateau region near the critical point is intimately related to the correlation length of the density fluctuations. However, the overall changes in vibrational lifetime seen in the different SCF solvents can be discussed in terms of experiments and theory used to address vibrational relaxation in liquids. $W(CO)_6$ has a lifetime of 700 ps in room temperature CCl_4, 350 ps in $CHCl_3$, and 150 ps in 2-methylpentane.[18–20] This trend has been discussed in terms of a fully quantum-mechanical description of the force correlation function.[19] The bath is taken to be harmonic and all orders of anharmonic relaxation processes are considered. The variations in lifetime with solvent can arise from the high-frequency modes available in the solvent, which determine the order of the relaxation process.[18–20] In CCl_4, a fifth-order process occurs, i.e., there are five creation and annihilation operators. The initial vibration is annihilated, three high-frequency solute–solvent modes are created, and a mode of the liquid's continuum (INM or fluid phonon) is created/annihilated. The latter is required to conserve energy in the overall process. When the solvent is changed to $CHCl_3$, a C–H bending mode at ~ 1250 cm^{-1} becomes available for the relaxation path. This may lower the order of the process to fourth order, and the lifetime is substantially faster. In 2-methylpentane, there are more intermediate frequency modes available. Since additional modes can provide a more efficient pathway for relaxation,[18–20] the lifetime is even faster. At a given density in a SCF solution, these same considerations will apply. The change in lifetime in progressing from CO_2 to fluoroform to ethane is indicative of the important role played by the molecular properties of the SCF solvent in vibrational relaxation.

B. Vibrational frequency shifts

A plot of vibrational line center frequency of the $W(CO)_6$ T_{1u} mode versus CO_2 solvent density is shown in Fig. 6 for the 33 and 50 °C isotherms. The density dependence of the vibrational frequency shifts is remarkably similar to that of the vibrational lifetime at both temperatures. The line center frequency data also shows three readily identifiable types of behavior along the $T_r \approx 1.01$ isotherm: (1) a smoothly varying redshift with increasing solvent density for values of ρ_r below about 0.8, (2) a plateau region centered about ρ_c, and (3) the resumption of a gradual redshift for increasing values of the density above $\rho_r \sim 1.2$.

The density independence of the vibrational line frequency near ρ_c vanishes when the temperature is raised to 50 °C. Both the vibrational lifetime data shown in Figs. 2 and 3 and the line center frequencies in Fig. 6 display the same trends across the entire range of densities at the two temperatures. The similarity in the behavior of the two vibrational observables strongly suggests a common origin.

Vibrational frequency shift data for dilute mixtures of $W(CO)_6$ in ethane is shown in Fig. 7. Again, for the isotherm close to the critical temperature, a density-independent plateau is observed, while at 18 °C above the T_c, the plateau is not present. Both CO_2 and ethane are nonpolar solvents,

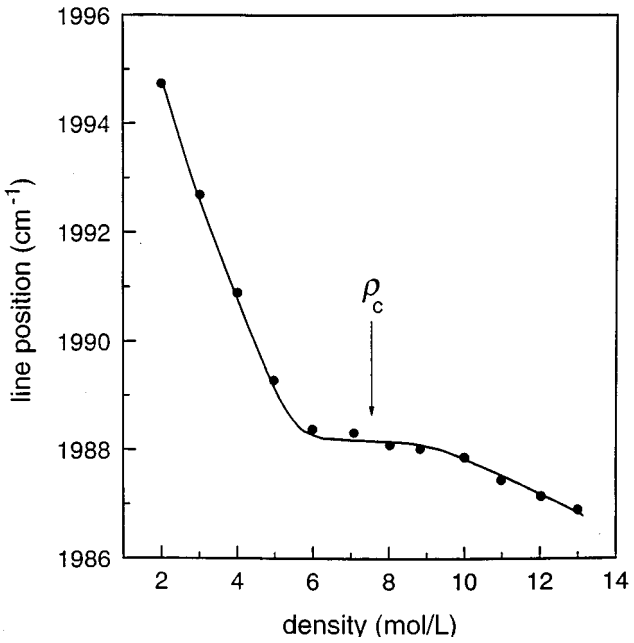

FIG. 8. Absorption line peak position of the T_{1u} asymmetric CO stretching mode of $W(CO)_6$ versus density of CHF_3 at 28 °C. The line through the data is a visual aid. The critical density is marked by an arrow.

whereas fluoroform is highly polar. Figure 8 displays spectral shift data for $W(CO)_6$ in fluoroform. Like the lifetime data of Fig. 5, the spectral shift data display a plateau around ρ_c along the 28 °C isotherm.

The possibility that these observations are due to some property of the $W(CO)_6$ solute molecule was tested by performing spectral shift measurements on the symmetric CO stretch of $Rh(CO)_2$acac. Figure 9(a) presents the vibrational line position data for the solute $Rh(CO)_2$acac in supercritical CO_2 at 33 °C. The vibrational frequency displays a pronounced plateau about ρ_c, with both the pre- and post-plateau regions of density exhibiting the familiar smooth variations in line shifts observed for $W(CO)_6$ in CO_2, ethane, and fluoroform. Finally, vibrational line position data taken for the $Rh(CO)_2$(acac)/ethane system are shown in Fig. 9(b) at 34 °C. Again, there is a well-defined plateau for the isotherm near T_c. In addition, the line positions of the asymmetric CO stretch at ~2020 cm^{-1} displayed this same dependence on density. Two solute molecules in three SCF solvents have been examined. The vibrational lifetime data and/or the vibrational line shift data all display a density-independent region around ρ_c on isotherms very near T_c. On isotherms about 20 °C above T_c, all data display continuous changes with density. The results indicate that the effect does not arise because of the characteristics of a particular solute–solvent system. The density independence of both microscopic vibrational observables in the vicinity of the critical point suggests that the phenomena are related to the long wavelength density correlations that occur near a critical point.

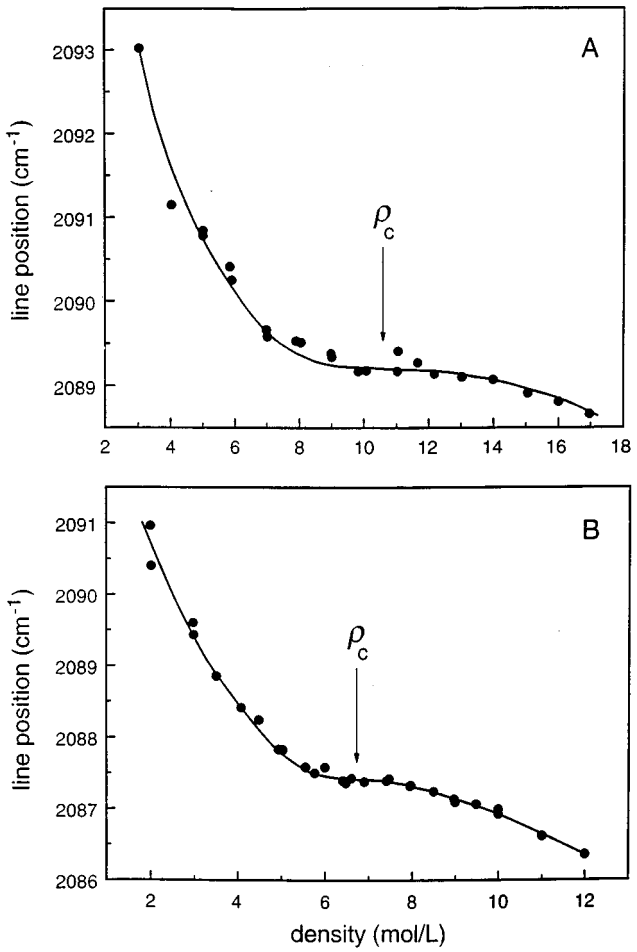

FIG. 9. (A) Absorption line peak position of the symmetric CO stretching mode of $Rh(CO)_2$acac versus density of CO_2 at 33 °C. (B) Same type of data as shown in (A), but here the solvent is C_2H_6 at 34 °C. The lines through the data are visual aids. The critical densities are marked with arrows. The presence of a plateau about ρ_c in both line position vs density plots implies that this effect does not depend on the identity of the solute.

IV. THEORY

From the striking resemblance of the lifetime curves in Figs. 2–5 to the $P-V$ isotherms of real gases, it is tempting to speculate that the occurrence of a process akin to condensation (clustering of the solvent around the solute in a type of local condensation) is the reason why vibrational lifetimes of $W(CO)_6$ do not decrease smoothly with solvent density near the critical isotherm. In this picture, the initial ''noncritical'' (low-density) portions of the lifetime curves reflect the increase with density of molecular interactions responsible for relaxation of the vibrationally excited species. The intermediate plateau exists because of a local phase transition to some kind of solute-solvent cluster. Analogous behavior in real gases is well understood as corresponding to liquefaction. However, as discussed below, *clustering is not required to explain the data*.

While the cluster model is appealing and has often been invoked in studies of so-called attractive supercritical mixtures,[21] it is by no means clear that it is the only explanation of the available data. It is quite possible that critical

fluctuations alone produce the anomalies seen near the critical point. Moreover, the results of the experiments indicate a degree of universality in the curves of lifetime versus density and spectral shift versus density that are somewhat at odds with a model that relies on the effects of specific intermolecular interactions. We have now developed a theory of vibrational relaxation and vibrational spectral shifts in supercritical fluids that actually points to the irrelevance of clustering, and to the importance of critical phenomena, as an explanation of our observations.[2] In fact, the theory suggests, among other things, that similar vibrational data are likely to be obtained even in pure fluids, or in repulsive supercritical mixtures. (The theory does not rule out the importance of clustering in other contexts.) Details of the theory are discussed elsewhere,[2] but its broad outlines are presented below.

A. Lifetimes

The CO asymmetric stretching mode of $W(CO)_6$ is modeled as a harmonic oscillator of natural frequency ω that is in contact with a thermal reservoir at temperature T representing the molecules of the surrounding solvent. The characteristic decay time T_1 for dissipation of excess vibrational energy from the first excited state of the oscillator to the medium can be shown to have the following form:[2,22,23]

$$T_1^{-1}=\frac{\beta}{m}\int_0^\infty dt\langle F(t)F(0)\rangle_{\mathrm{cl}}\cos(\omega t). \tag{1}$$

Here, m is the reduced mass of the oscillator, and β is $1/k_BT$, where k_B is Boltzmann's constant. $F(t)$ is the fluctuating force on the oscillator in one dimension (the normal coordinate of the mode) at time t, and the angular brackets denote a classical equilibrium average over the solvent degrees of freedom.

The force correlation function that appears in Eq. (1) is calculated using density functional theory,[2,24–26] which expresses the Helmholtz free energy A of the system as a functional Taylor's expansion in the local density fluctuations of its components, $\rho_i(\mathbf{r},t)-\rho_i^0$, where i refers to solvent ($i=1$) or solute ($i=2$), and ρ_i^0 is the mean density of that component. The fluctuating force $\mathbf{F}_i(\mathbf{r},t)$ on i at $\mathbf{r}$ and t is then defined as the negative gradient of the effective potential at $\mathbf{r}$ and t, which in turn in related to the functional derivative of A with respect to $\rho_i(\mathbf{r},t)$.[2,26] The force correlation function in Eq. (1) above is then identified as the integral over $\mathbf{r}$ of $\langle\mathbf{F}_i(\mathbf{r},t)\cdot\mathbf{F}_i(\mathbf{r},0)\rangle$. Eventually it can be shown that[2]

$$T_1^{-1}\propto T\int_0^\infty dt\,\cos(\omega t)\int d\mathbf{k}\,\mathbf{k}^2|\hat{C}_{12}(\mathbf{k})|^2\hat{S}_1(\mathbf{k},t). \tag{2}$$

Here, $\mathbf{k}$ is a wave vector in 3-space, $\hat{C}_{12}(\mathbf{k})$ is the direct correlation function between solute and solvent, and $\hat{S}_1(\mathbf{k},t)$ is the dynamic structure factor of the solvent. The derivation of Eq. (2) neglects density fluctuations at third order and beyond; this is generally valid in the study of dense liquids, and may well be valid for liquids near the critical point as well, since the associated three and higher particle direct correlation functions are likely to be small. Various constants independent of temperature and density have been omitted in Eq. (2).

Neither $\hat{C}_{12}(\mathbf{k})$ nor $\hat{S}_1(\mathbf{k},t)$ is known in general, so they are approximated. In the noncritical region, $\hat{C}_{12}(\mathbf{k})$ is described by the direct correlation function of a binary hard sphere mixture, (for which an exact expression is available from the solution to the Ornstein–Zernike equation[27]) while in the critical region it is described by certain scaling relations known to be applicable there.[28] In the same spirit, $\hat{S}_1(\mathbf{k},t)$ is obtained from an extended hydrodynamic description, and is written as[2,29]

$$\hat{S}_1(\mathbf{k},t)=\hat{S}_1(\mathbf{k})e^{-t/\tau(\mathbf{k})}\left(1+\hat{P}_1(\mathbf{k})\right), \tag{3}$$

where $\hat{S}_1(\mathbf{k})$ is the static structure factor of the solvent, $\tau(\mathbf{k})$ is a characteristic wave vector dependent decay constant, and $\hat{P}_1(\mathbf{k})$ is a term that accounts for acoustic phonons in the medium. $\hat{S}_1(\mathbf{k})$, $\tau(\mathbf{k})$, and $\hat{P}_1(\mathbf{k})$ are themselves further approximated: $\hat{S}_1(\mathbf{k})$ by the Ornstein–Zernike equation,[2,30] $\tau(\mathbf{k})$ by the Kawasaki equation,[2,29,31,32] and $\hat{P}_1(\mathbf{k})$ by a function described in Ref. 2.

Equation (2) is first evaluated in the limit $\mathbf{k}\xi\ll 1$, ξ being the correlation length of density fluctuations. In this limit,[29] which corresponds to the noncritical region of the phase diagram, $1/\tau(\mathbf{k})\approx D_T\mathbf{k}^2$, where D_T is the thermal diffusivity of the solvent, and $\hat{S}_1(\mathbf{k})\approx\rho_1\kappa_T/\kappa_T^0$, where ρ_1 is the number density of the solvent, κ_T is its isothermal compressibility and κ_T^0 is the isothermal compressibility of the ideal gas. Approximating $\hat{C}_{12}(\mathbf{k})$ by its $\mathbf{k}=0$ value (which has been shown to be a reasonable approximation[2]), and omitting all physical constants that are independent of the temperature and density, the lifetime is given by

$$T_1^{-1}\propto T\rho_1\frac{\kappa_T}{\kappa_T^0}\hat{C}_{12}(0)^2Q, \tag{4}$$

where Q is a complicated analytical function containing thermodynamics functions such as κ_T and D_T defined in Ref. 2.

The temperature and density dependence of Eq. (4) (the noncritical limit) is determined by the temperature and density dependence of ξ, κ_T, D_T, and $\hat{C}_{12}(0)$, of which only the last has a relatively simple analytic form (for the hard sphere model, there is no temperature dependence as such). Although ξ, κ_T, and D_T are not known in general as functions of ρ and T, experimental data on specific solvents (including carbon dioxide and ethane) have been used to fit them to polynomial and exponential expansions in these variables.[33,34] We use the fitted expressions for ethane[34] to determine the isotherms of T_1 (the expression for carbon dioxide is significantly more complicated), two of which are shown in Fig. 10(a) for densities in the range of 1 to 5 mol/L. The curve with the longer lifetime at the lowest density corresponds to $T=34$ °C and the other curve to $T=52$ °C. The critical temperature of ethane is 32.2 °C and the critical density is 6.87 mol/L.

In obtaining these plots, several of the model parameters of our theory (including the solute and solvent diameters, the

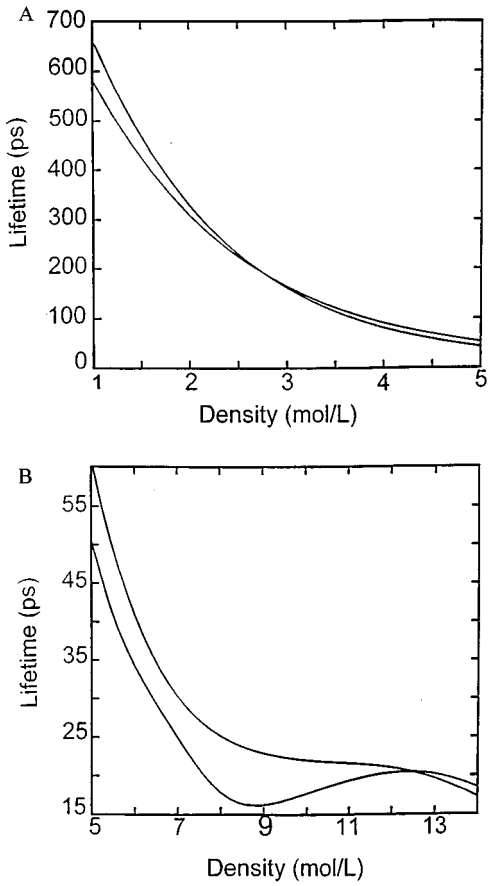

FIG. 10. (A) Vibrational lifetime vs density as calculated from Eq. (4) for densities in the range of 1–5 mol/L at temperatures of 34 and 52 °C. The curve with the larger lifetime at a density of 1 mol/L corresponds to the 34 °C isotherm. (B) Vibrational lifetime vs density as calculated from Eq. (4) for densities in the range of 5–14 mol/L at 34 and 52 °C. The curve with the minimum corresponds to the 34 °C isotherm.

frequency and mass of the oscillator, and the cut-off on high momenta) have been assigned physically reasonable values.[2] Being independent of density and temperature, they do not affect the final results, except for numerical factors. We have also scaled the plots so that at the lowest measured concentration (1 mol/L), the predicted and experimental lifetimes roughly coincide.

As is evident, Eq. (4) reproduces the *qualitative* features of the experimental data at both temperatures in the low density region, although the predicted lifetime decays are faster than is actually the case. If Eq. (4) is applied to the near-critical region ($T \approx T_c$, $5 < \rho < 10$ mol/L), the results are as shown in Fig. 10(b), which also includes the $T = 52$ °C isotherm for comparison, and densities in the range $\rho > 10$ mol/L. Not surprisingly, the equation breaks down in the vicinity of the critical point, but it does show the expected decay of the lifetime along the near-critical isotherm at high densities ($\rho > 11$ mol/L). The isotherm at $T = 52$ °C decays continuously with density, which is the behavior observed experimentally for both CO_2 and ethane.

To probe the region near the critical point, we not consider the limit $\mathbf{k}\xi \gg 1$. In this limit,[2,29] $\tau(\mathbf{k}) \approx D_T \xi \mathbf{k}^3$, and the contribution from $\hat{P}_1(\mathbf{k})$ is negligible. The lifetime itself becomes [omitting constant $\hat{S}_1(\mathbf{k}) \approx \rho_1 \kappa_T / \kappa_T^0 \mathbf{k}^2 \xi^2$ is independent of the density and temperature as before]

$$T_1^{-1} \propto T \frac{\rho_1 \kappa_T / \kappa_T^0}{\xi^2} \hat{C}_{12}(0)^2 \int_0^\infty dt \cos(\omega t) \int d\mathbf{k} \times \exp(-D_T \xi \mathbf{k}^3 t). \tag{5}$$

All the symbols in this equation have their earlier definitions.

Several conclusions can be drawn from this expression without actually evaluating the integral explicitly. It is known from scaling arguments that both $\rho_1 \kappa_T / \kappa_T^0 \xi^2$ and $D_T \xi$ virtually independent of the density.[2] Hence, the density dependence of T_1, if it exists at all, must come from $\hat{C}_{12}(0)$. But it can be shown from the fluctuation theory of Kirkwood and Buff,[28] that for infinitely dilute binary mixtures $\hat{C}_{12}(0)$ asymptotically approaches a constant as $T \to T_c$ and $\rho \to \rho_c$. Thus all parameters that give rise to a density dependence away from the critical point scale out of the problem near the critical point. T_1, therefore, becomes essentially density independent.

These theoretical results are in accord with the experimental data. Following the presentation of the theory of the frequency shift, a discussion of the results will be presented. However, it is important to note that the theory did not explicitly include any type of clustering phenomena. The theory did include the long wavelength nature of the density correlations near the critical point, and it implicitly averages over regions of high, intermediate, and low density. There is nothing in the calculations that places the solutes exclusively in the regions of high density. Therefore, the fact that there are correlated regions of high density should not be construed as ''clusters'' that give rise to the theoretical results.

B. Frequency shifts

Changes in the positions of absorption maxima on going from gas to liquid are generally attributed to forces in the condensed-phase medium that usually shift vibrational frequencies towards the red. Accordingly, if it is assumed that the shift $\Delta\nu$ between the observed liquid-phase frequency of the solvent ν and a putative gas-phase frequency ν_g (which can be regarded as the extrapolated zero concentration limit of the liquid-phase frequency) is related to the averaged force on the vibrational coordinate of interest, it can also be shown[2] that

$$(\Delta\nu)^2 \propto T^2 \int d\mathbf{k}\, k^2 |\hat{C}_{12}(\mathbf{k})|^2 \hat{S}_1(\mathbf{k}). \tag{6}$$

In the noncritical limit, this becomes

$$(\Delta\nu)^2 \propto T^2 \rho_1 \frac{\kappa_T}{\kappa_T^0} \hat{C}_{21}(0)^2 \frac{1}{\bar{\Lambda}^2} \left(1 - \frac{3}{\bar{\Lambda}^2} + \frac{3}{\bar{\Lambda}^3} \tan^{-1} \bar{\Lambda} \right), \tag{7}$$

where $\bar{\Lambda} \cong \Lambda \xi$, with Λ a cut-off on high momenta. In the critical limit, Eq. (6) becomes

$$(\Delta\nu)^2 \propto T^2 \frac{\rho_1 \kappa_T/\kappa_T^0}{\xi^2} \hat{C}_{12}(0)^2. \tag{8}$$

Equation (7) gives a redshift for densities well above or below the critical density.[2] It also comes close to quantitatively reproducing the overall magnitude of the frequency shift with density.[2] However, for densities and temperatures close to the critical point, Eq. (8), which is the appropriate equation, is essentially density independent. As above, $\rho_1 \kappa_T/\kappa_T{}^0$ scales as ξ^2 and $\hat{C}_{12}(0)$ becomes virtually independent of density near the critical point. The net result is that Eq. (8) predicts the plateau in frequency shifts observed in the data near the critical point.

V. DISCUSSION

The theory outlined above is based on a thermodynamic description of the interactions of a solute vibration with the SCF solvent. This approach was used to provide an analysis that was capable of including the known scaling of physical phenomena near the critical point. A thermodynamic formulation of vibrational relaxation cannot be expected to reveal fully how vibrational energy is transferred from solute to solvent when the system moves from noncritical to critical environments, because it does not include a molecular-level picture of interactions and dynamics, but what appears to happen is as follows. Initially, as the density of the solvent is increased along an isotherm near the critical temperature, the solute encounters many more nearby neighbors. The increase in intermolecular interactions will increase the probability that the solute will dissipate energy to the medium and/or to lower frequency modes of the solute itself; its lifetime therefore tends to decrease. At the same time, the compressibility of the solvent starts to rise. The ability of the solute to exert a force on the solute therefore falls, and its lifetime accordingly will tend to increase. [This can be calculated using the full version of Eq. (4) in Ref. 2.] Thus there are counteracting effects. However, away from the critical point, the change in compressibility of the solvent is small, and not expected (initially) to offset the influence of the increased number of solvent molecules which interact with the solute.

Additionally, the diffusivity of the solvent decreases, which implies, rather crudely, that its capacity to receive energy is diminished. This effect also tends to increase lifetimes, but again, away from the critical point, the changes in D_T are small enough initially as not to be unduly important. These trends can be derived from Eq. (4) in the limit $\xi \to 0$. In this limit, both κ_T and D_T are reasonably approximated by their ideal gas values. This means that $\kappa_T/\kappa_T^0 \to 1$, and that D_T is not strongly density dependent. Very roughly then, $T_1 \sim 1/\hat{C}_{12}(0)^2 \rho_1$. Now $\hat{C}_{12}(0)$ for the binary hard sphere model becomes more negative with density (the density dependence is actually very slight). $\hat{C}_{12}(0)^2$ increases, so the net effect is that at constant temperature and away from the critical point, the rate of vibrational decay is largely a function only of the number of molecules that surround the solute in its immediate vicinity.

As critical fluctuations develop at still higher densities, new effects come into play. The compressibility now grows dramatically. If this were all that happened, then for the reasons indicated earlier, T_1 would increase. But the growth of κ_T is also accompanied by a growth in the correlation length ξ, which corresponds to the range over which molecules of the solvent are—loosely speaking—''in phase'' with each other. This means that despite the greater ease with which the solute can push aside its neighbors during the course of its oscillatory motion, many more of them are now present in the correlated volume of space that bears down on it. If this volume is regarded as a sphere of radius ξ, the number of *additional* solvent molecules that act in concert on the solute varies roughly as ξ^2, the area of a sphere of this radius. Because of the way κ_T and ξ scale with density near the critical point, these two opposing effects compensate each other.

The diffusivity also changes dramatically, but it tends to vanish rather than diverge. The vanishing of D_T is essentially a consequence of the divergence of the heat capacity, to which it is inversely related. In physical terms, the molecules of solvent that surround the solute in a sphere of radius ξ act as an energy reservoir (bath) of large heat capacity. Thus, although D_T decreases (and it can be shown that it decreases essentially inversely as the linear dimensions of the reservoir), its decrease is almost exactly matched by the growth of ξ. Thus neither a change in compressibility nor in diffusivity affects T_1, so long as the system is near the critical point. This leaves the direct correlation function as the sole remaining source of potential density dependence in T_1. As stated earlier, $\hat{C}_{12}(0)$ is not strongly dependent on density. As the critical point is approached, it asymptotically reaches a constant value.

In summary, the numerous microscopic degrees of freedom into which vibrational modes of excitation can relax, and which remain unseen in a classical description, are described by bulk properties of the system that have very definite, measurable effects near the critical point. While the parameters, ρ, κ_T, D_T, and ξ are all changing dramatically, they combine in a manner that leaves the vibrational lifetime and frequency shift independent of density. It is important to note that the results are not a function of some special environment for the solutes. In fact, the theory predicts density-independent plateaus for repulsive as well as attractive solute–solvent interactions. It also can be applied to pure SCFs[2] and predicts plateaus for vibrational observables in pure SCFs.

The theory demonstrates that it is possible to account for plateaus without invoking a form of clustering, i.e., condensation of solvent molecules around the solute. Experiments on solute–solvent partial molar volumes in which very large negative partial molar volumes have been observed[3,4] have been used to suggest the existence of clusters in some systems.[5,35–37] However, theoretical treatments indicate that the results of the partial molar volume experiments may arise primarily because of the long correlation lengths and large compressibility near the critical point rather than a type of liquidlike condensation/clustering of solvent molecules

around a solute.[38,39] The combined experimental and theoretical results presented here do not imply that solute–solvent clusters cannot exist. What the theory *does* show is that the plateaus in the data can be explained as a manifestation of critical phenomena. The density-independent observables arise because of the dramatic growth in correlation length near the critical point.

The large correlation length near the critical point not only results in the plateaus, but it also enhances the normal density-dependent trends. This can be seen most clearly in Fig. 4, where for fixed density near ρ_c, the lifetime actually becomes longer when the temperature is increased from 34 to 50 °C. In Fig. 6, at fixed density near ρ_c, the frequency shifts to the blue as T is increased. In an experimental and theoretical treatment which will be presented subsequently, it will be shown that the constant density lifetime continues to increase, until a turnaround temperature is reached, after which the lifetime decreases. The theory presented here can describe this behavior.

VI. CONCLUDING REMARKS

In this paper, we have presented a study of vibrational dynamics of polyatomic solutes in polyatomic SCFs over a range of densities and temperatures, including the region around the critical point. The data for two solutes in three SCFs show very well-defined density-independent regions on isotherms close to T_c.

Other types of density-independent observables in SCFs have been reported previously. Sun, Fox, and Johnston[5] examined the density dependence of the electronic spectral shifts for *p*-(*N*,*N*-dimethylamino)benzonitrile and ethyl *p*-(*N*,*N*-dimethylamino)benzoate in supercritical fluoroform, carbon dioxide, and ethane. A notable feature of their data is the presence of a density-independent plateau in the spectral shifts in the near-critical region. The plateau was reported as evidence for solute–solvent clustering.

Bennett and Johnston[7] measured the peak shifts in the electronic absorbance bands of benzophenone and acetone. They observed the peak positions to be independent of density in supercritical water near the critical point. This effect was especially prominent in the case of the acetone/water system, and was attributed primarily to hydrogen bonding. The existence of a plateau in the near-critical region was taken as an indication of the existence of solute–solvent clusters.

Carlier and Randolph[6,40] used electron paramagnetic resonance spectroscopy to investigate stable ditertbutyl nitroxide (DTBN) radicals in supercritical ethane. They measured the nitrogen hyperfine-splitting constant $(A_N(G))$.[6] The shape of the $A_N(G)$ vs ρ_r plot at $T_r = 1.009$ exhibits a plateau region. Data taken along the $T_r = 1.084$ isotherm shows that the plateau vanishes at higher temperature. Calculation of the local density enhancement about the DTBN radical as a function of bulk ethane density yields the conclusion that the maximum local density of roughly 12 mol/L does *not* occur at ρ_c, where $A_N(G)$ is density independent, but rather at $\sim \rho_c/2$. Carlier and Randolph explains this result in terms of a prewetting transition similar to that observed for ultrapure argon in the vicinity of a platinum surface.[41] They suggest that short-ranged forces between ethane and DTBN cause a filling of at least the first solvent shell about the radical to liquidlike ethane densities (~12 mol/L), and emphasize that this effect does not require the presence of long-ranged density fluctuations. It is then argued that clustering, i.e., local density augmentation, in supercritical fluid solutions depends on local considerations of solvent structure rather than the involvement of any critical phenomena.

The preliminary report of data of the type presented here[1] also described the density independence of the vibrational observables in terms of clusters. It is tempting to say that since there is no density dependence, the local density experienced by the solute must not be varying, even if the bulk density is changing, i.e., a solute–solvent cluster is formed. However, for the vibrational measurements discussed here, the theory shows that solute–solvent clustering is unnecessary to explain the observations. Rather, the observations involve a play-off among rapidly changing properties of the system near the critical point that leads to the lack of density dependence. Clusters may indeed exist, but the results show that a detailed calculation of observables, which does not build solute–solvent clusters into the theory, can explain the data. The theory implicitly averages over all solute environments, regions of both high and low density, to produce the final, density-independent results.

The word cluster has a variety of meanings when SCFs are discussed. In a pure SCF near the critical point, there are regions with long correlation lengths of high, average, and low density. Frequently, the regions of high density are described as clusters. Near the critical point, the long correlation lengths give rise to anomalous thermodynamic properties, e.g., the very large isothermal compressibility. The interplay of the anomalous thermodynamic properties of the solvent near the critical point is associated with the plateau in the vibrational observables. If regions of large correlation length are considered clusters, then clusters are involved in the observed behavior. However, the theory described above and in more detail in Ref. 2 explains the data without invoking any particular aggregation of the solvent around the solute resulting from attractive solute–solvent interactions.

The experiments demonstrate the sensitivity of vibrational observables to the correlation length of density fluctuations. Large correlation lengths have a significant effect on vibrational dynamics. The experiments and theory are a step towards understanding the influence of correlation length on vibrational dynamics in SCFs near the critical point.

ACKNOWLEDGMENTS

This work is supported by the Air Force Office of Scientific Research (F49620-97-1-0061). B.J.C. gratefully acknowledges the Office of Naval Research (N00014-96-1-0809) for financial support during his sabbatical visit to

Stanford. D.J.M. and P.H.D. thank the National Science Foundation for assistance through the Graduate Research Fellowship program.

[1] R. S. Urdahl, K. D. Rector, D. J. Myers, P. H. Davis, and M. D. Fayer, J. Chem. Phys. **105**, 8973 (1996).
[2] B. J. Cherayil and M. D. Fayer, J. Chem. Phys. (submitted).
[3] C. A. Eckert, D. H. Ziger, K. P. Johnston, and T. K. Ellison, Fluid Phase Equilib. **14**, 167 (1983).
[4] C. A. Eckert, D. H. Ziger, K. P. Johnston, and S. Kim, J. Phys. Chem. **90**, 2738 (1986).
[5] Y.-P. Sun, M. A. Fox, and K. P. Johnston, J. Am. Chem. Soc. **114**, 1187 (1992).
[6] C. Carlier and T. W. Randolph, AIChE J. **39**, 876 (1993).
[7] G. E. Bennett and K. P. Johnston, J. Phys. Chem. **98**, 441 (1994).
[8] M. Lee, G. R. Holtom, and R. M. Hochstrasser, Chem. Phys. Lett. **118**, 359 (1985).
[9] D. E. Smith and C. B. Harris, J. Chem. Phys. **87**, 2709 (1987).
[10] A. L. Harris, J. K. Brown, and C. B. Harris, Annu. Rev. Phys. Chem. **39**, 341 (1988).
[11] M. E. Paige and C. B. Harris, J. Chem. Phys. **93**, 1481 (1990).
[12] M. E. Paige and C. B. Harris, Chem. Phys. **149**, 37 (1990).
[13] C. Lienau and A. H. Zewail, J. Phys. Chem. **100**, 18 629 (1996).
[14] A. Materny, C. Lienau, and A. H. Zewail, J. Phys. Chem. **100**, 18 650 (1996).
[15] Q. Liu, C. Wan, and A. H. Zewail, J. Phys. Chem. **100**, 18 666 (1996).
[16] D. Schwarzer, J. Troe, M. Votsmeier, and M. Zerezke, J. Chem. Phys. **105**, 3121 (1996).
[17] A. Tokmakoff, C. D. Marshall, and M. D. Fayer, JOSA B **10**, 1785 (1993).
[18] A. Tokmakoff, B. Sauter, and M. D. Fayer, J. Chem. Phys. **100**, 9035 (1994).
[19] V. M. Kenkre, A. Tokmakoff, and M. D. Fayer, J. Chem. Phys. **101**, 10 618 (1994).
[20] P. Moore, A. Tokmakoff, T. Keyes, and M. D. Fayer, J. Chem. Phys. **103**, 3325 (1995).
[21] C. A. Eckert, B. L. Knutson, and P. G. Debenedetti, Nature **383**, 313 (1996).
[22] J. S. Bader and B. J. Berne, J. Chem. Phys. **100**, 8359 (1994).
[23] S. A. Egorov and J. L. Skinner, J. Chem. Phys. (to be published).
[24] T. Munakata, J. Phys. Soc. Jpn. **45**, 749 (1978).
[25] T. R. Kirkpatrick and J. C. Niewouldt, Phys. Rev. A **33**, 2651 (1986).
[26] B. Bagchi, J. Chem. Phys. **100**, 6658 (1994).
[27] J. L. Lebowitz, Phys. Rev. **133**, 895 (1964).
[28] J. G. Kirkwood and F. P. Buff, J. Chem. Phys. **19**, 774 (1951).
[29] D. L. Henry, H. L. Swinney, and H. Z. Cummins, Phys. Rev. Lett. **25**, 1170 (1970).
[30] D. A. McQuarrie, *Statistical Thermodynamics* (University Science Books, Mill Valley, 1973).
[31] K. Kawasaki, Ann, Phys. **61**, 1 (1970).
[32] R. A. Ferrell, Phys. Rev. Lett. **24**, 1169 (1970).
[33] V. Vesovic, W. A. Wakeham, G. A. Olchowy, J. V. Sengers, J. T. R. Watson, and J. Millat, J. Phys. Chem. Ref. Data **19**, 763 (1990).
[34] D. G. Friend, H. Ingham, and J. F. Ely, J. Phys. Chem. Ref. Data **20**, 275 (1991).
[35] P. G. Debenedetti, Chem. Eng. Sci. **42**, 2203 (1987).
[36] M. P. Heitz and F. V. Bright, J. Phys. Chem. **100**, 6889 (1996).
[37] S. Kim and K. P. Johnston, AIChE J. **33**, 1603 (1987).
[38] I. G. Economou and M. D. Donohue, AIChE J. **36**, 1920 (1990).
[39] D. B. McGuigan and P. A. Monson, Fluid Phase Equilib. **57**, 227 (1990).
[40] T. W. Randolph and C. Carlier, J. Phys. Chem. **96**, 5146 (1992).
[41] G. Ascarelli and H. Nakanishi, J. Phys. (Paris) **51**, 341 (1990).